Journal of Applied Polymer Science

Photocuring of Cycloaliphatic Epoxy Formulations Using Polyesters with Multiarm Star Topology as Additives

Marjorie Flores,[1] Xavier Fernández-Francos,[1] Xavier Ramis,[2] Marco Sangermano,[3] Francesc Ferrando,[4] Àngels Serra[1]

[1]Department of Analytical and Organic Chemistry, Universitat Rovira i Virgili, C/ Marcel·lí Domingo s/n, 43007, Tarragona, Spain
[2]Thermodynamics Laboratory, ETSEIB Universitat Politècnica de Catalunya, Av. Diagonal 647, 08028, Barcelona, Spain
[3]Department of Material Science and Chemical Engineering, Politecnico di Torino, C.so Duca degli Abruzzi 24, 10129 Torino, Italy
[4]Department of Mechanical Engineering, Universitat Rovira i Virgili, C/ Països Catalans, 26, 43007, Tarragona, Spain
Correspondence to: X. Fernández-Francos (E-mail: xavier.fernandez@urv.cat)

ABSTRACT: Multiam star polyesters were synthesized by growing poly(ε-caprolactone) (PCL) arms from hyperbranched polyesters cores of different molecular weight and used as polymeric modifiers in UV-curable cationic formulations based on a biscycloaliphatic epoxy resin. The effect of the multiarm stars on the curing kinetics has been investigated by real-time FTIR. The thermal-mechanical properties of the photocured thermosets have been studied with calorimetry and dynamomechanical and thermogravimetric analysis. Impact strength tests have been performed to assess their effect on the toughness of the cured materials. An accelerative effect of these modifiers has been observed as a consequence of the participation of the hydroxyl groups of the modifiers in the cationic curing of the epoxy resin. A modest increase in toughness accompanied by a decrease in the glass transition are observed, as a consequence of the incorporation of the modifiers into the network structure, leading to homogeneous, *in situ* reinforced materials. © 2013 Wiley Periodicals, Inc. J. Appl. Polym. Sci. **2014**, *131*, 40005.

KEYWORDS: hyperbranched polymers; multiarm stars; thermosets; photopolymerization

Received 5 July 2013; accepted 22 September 2013
DOI: 10.1002/app.40005

INTRODUCTION

The widespread use of thermosetting epoxy resins in many industrial applications such as coatings, adhesives, molding compounds, or composites, can be explained by a combination of attractive properties, such as their thermomechanical behavior, their chemical and environmental stability and their good processability.[1] In addition, they are highly versatile because of the great variety of available curing agents and organic and inorganic modifiers and fillers that can be used to improve their properties.[2] Bisphenol A resins are by far the most widely used epoxy resins, but cycloaliphatic epoxy resins possess some superior properties such as high arc resistance, low viscosity, high heat deflection temperatures, and excellent weatherability,[1] which make them a better choice depending on the application, such as photocurable cationic formulations.[3–6] However, a major drawback of cycloaliphatic epoxy resins is their brittleness, caused to their high crosslinking density, and the rigidity of the polymeric backbone, which may place strong restrictions and design constraints in their application.[7]

Liquid rubbers and thermoplastics were firstly used as additives to increase the fracture toughness of thermosets but the thermomechanical properties and the processability is greatly compromised.[8] Recently, hyperbranched polymers (HBP) have been proposed as alternative polymeric modifiers for thermosetting formulations.[9–13] The dendritic structure of HBPs makes these modifiers very promising in terms of processability because of the low entanglement that leads to low viscosities in comparison to linear polymers.[14] By partial or complete modification of their numerous hydroxyl terminal groups, it is possible to tune their interaction with the matrix or facilitate their covalent linkage to the epoxy matrix, which can lead to phase-separated or homogeneous morphologies.[15,16] The presence of non-modified reactive groups in the HBP shell can improve the interaction in the interphase between the separated particles and the matrix.

The reports on the toughening of cycloaliphatic epoxides are scarce and the field is still open for research. A variety of modifiers such as high-viscosity CTBN rubbers,[17,18] poly(ethylenephtalate),[19] inorganic fillers such as nanosize silicon dioxide[20]

or carbon nanotubes,[21] oligofluorosiloxanes,[22] reactive copolymers,[23] or multiarm hyperstars[24] have been tried with different degrees of success. We recently reported a two-fold increase in the impact strength of thermally cured cycloaliphatic epoxides using a hyperbranched poly(glycidol) partially modified with end undecenoyl chains.[16] The use of reactive hyperbranched polymers in the UV curing of cycloaliphatic epoxides has also been reported,[12,25–27] producing in most cases a toughness increase at the expense of reducing the glass transition temperature T_g and the elastic modulus.

Multiarm stars are another class of dendritic polymers that can be used as polymeric modifiers for epoxy thermosets, with similar advantages to those of hyperbranched polymers, because of their compact dendritic structures. Karger-Kocsis et al.[28] reported a significant toughness increase in vinyl ester–urethane hybrid formulations using hyperbranched star-like polyethers as modifiers. Morell et al.[29] synthesized multiarm stars with poly(ε-caprolactone) arms and hyperbranched poly(glycidol) core and used them in cationic epoxy formulations, which resulted in a significant increase in toughness. Acebo et al.[30] reported the synthesis of multiarm stars with poly(ε-caprolactone) arms and hyperbranched poly(ethyleneimine) core and their use in anionic epoxy formulations, showing a complex effect on the impact strength depending on the arm length and core size. Multiarm stars with hyperbranched aromatic-aliphatic polyester core and poly(methyl methacrylate-*b*-hydroxyethyl methacrylate) arms with different copolymeric sequence and composition have been used as polymeric modifiers in UV-cured and thermally cured biscycloaliphatic formulations,[24] but a decrease in both the strain at break and elongation at break were reported.

In this article, we report the synthesis modified Boltorn™ type hyperbranched polyesters of different core size modified by growing poly(ε-caprolactone) arms (HX-PCL) and used them in cationic UV-curable formulations based on a biscycloaliphatic epoxy resins (CE). The photocuring of these formulations has been monitored by real-time FTIR. The thermal and dynamo-mechanical properties have been measured using differential scanning calorimetry (DSC), thermogravimetric analysis (TGA), and dynamic-mechanic thermal analysis (DMTA). Mechanical tests have been performed to determine the impact strength of the resulting thermosets. The morphology of the materials has also been investigated by electron microscopy (SEM).

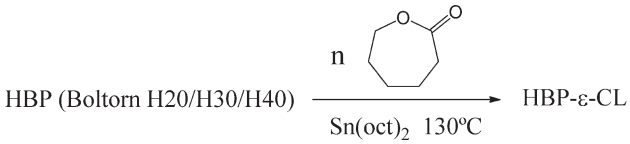

Scheme 1. Synthesis of multiarm stars with Boltorn cores and poly(ε-caprolactone) arms.

EXPERIMENTAL

Materials

The hyperbranched polymers Boltorn H20 ($M_w = 1747$ g/mol, 16 OH), Boltorn H30 ($M_w = 3500$ g/mol, 32 OH), and Boltorn H40 ($M_w = 7316$ g/mol, 64 OH) were donated by Perstorp and were used as received. ε-Caprolactone (ε-CL), distilled under vacuum, tin (II) 2-ethylhexanoate [$Sn(oct)_2$], bis-cycloaliphatic diepoxy resin 3,4-epoxycyclohexylmethyl 3,4-epoxycyclohexyl carboxylate (CE, 126 g/eq) and triphenylsulfonium hexafluoroantimonate (PI, $[Ph_3S]^+$ $[SbF_6]^-$) were purchased from Sigma-Aldrich.

Synthesis of Multiarm Stars (H20-PCL, H30-PCL, and H40-PCL) (Scheme 1)

About 5 g of the HBP and the required proportion of ε-CL in order to obtain 10 eq ε-CL per each eq OH of HBP (ratio 1 : 10 eqOH : ε-CL) (Table I) were mixed at room temperature in a two-necked flask with stirring under inert atmosphere.

Table I. Composition of the Formulations

	CE		HX-PCL		PI	
Formulation	X_{eq} ($\times 10^{-3}$)	Wt%	X_{eq} ($\times 10^{-5}$)	Wt%	X_{eq} ($\times 10^{-5}$)	Wt%
Neat	7.86	99.01	0.00	0.00	1.78	0.99
H20-PCL (%)						
5%	7.49	94.34	2.52	4.72	1.70	0.94
10%	7.15	90.09	4.81	9.01	1.62	0.90
20%	6.56	82.64	8.82	16.53	1.49	0.83
H30-PCL (%)						
5%	7.49	94.34	3.53	4.72	1.70	0.94
10%	7.15	90.09	6.75	9.01	1.62	0.90
20%	6.56	82.64	12.39	16.53	1.49	0.83
H40-PCL (%)						
5%	7.49	94.34	2.63	4.72	1.70	0.94
10%	7.15	90.09	5.02	9.01	1.62	0.90
20%	6.56	82.64	9.20	16.53	1.49	0.83

In percentage by total weight (%wt) of the mixture and equivalent ratio (X_{eq}) in eq/g of mixture of the relevant species.

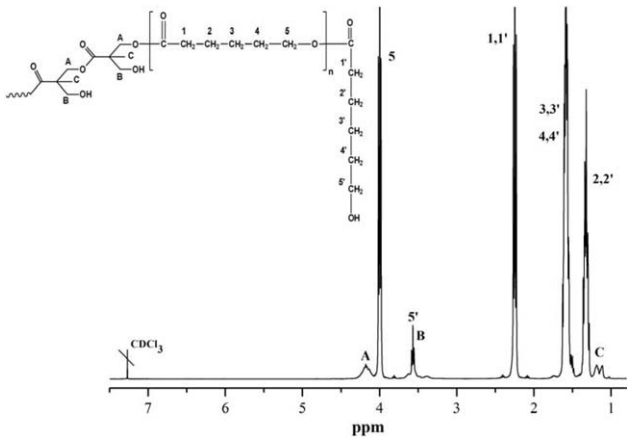

Figure 1. ^{1}H RMN spectrum of Boltorn H20 core modified with poly(ε-caprolactone) arms (H20-PCL) in $CDCl_3$.

Afterwards, the initiator ($Sn(oct)_2$) was added to the solution mixture and the flask was immersed in a thermostatic oil bath at 130°C during 24 h. Later, the product was precipitated in diethyl ether. Finally, the polymer was filtered and dried under vacuum at 45°C for 2 days. ^{1}H NMR (400 MHz, $CDCl_3$, ppm; Figure 1): 4.20 [–CH_2–O–CO–, (A)], 4.0 (–CH_2–OCO–, 5), 3.5 (–CH_2–OH, 5′), 3.30–3.70 [–CH_2–O– and –CH_2–OH, (B)], 2.20 (–CH_2–COO, 1 and 1′), 1.60–1.40 (–CH_2–, 3, 3′ and 4, 4′), 1.30 (–CH_2–, 2 and 2′), and 1.05–1.15 [–CH_3, (C)].

Sample Preparation

Mixtures were prepared by adding the required amount of HBP (5, 10, and 15 parts per hundred parts of resin, phr) to the epoxy resin (CE) and gently heating (*ca.* 80°C) until the HBP was dissolved and the solution became clear. After cooling down, 1 phr of the PI were added in reference to the CE resin (Table I) and the solution was homogenized by mechanical stirring. The structures of CE and PI and the idealized structure of the multiarm stars are shown in Scheme 2.

The samples were photocured in a UV oven (Vilber Lourmat Bio-Link Crosslinker) equipped with 6 lamps of 8 W each emitting 365 nm wavelength UV radiation. The samples for dynamic-mechanical thermal analyses (DMTA) (30 × 8 × 1 mm^3) were prepared by pouring the liquid formulation into a polypropylene mold with a 1 mm Teflon spacer. A dose of 12 J/cm^2 was applied on both sides of the samples in order to ensure complete activation of the photoinitiator. The samples for impact strength tests (25 × 12 × 2.5 mm^3) were photocured in a polypropylene mold with a 2.5 mm Teflon spacer. A dose of 36 J/cm^2 on each side of the samples was used in this particular case. After demolding, the samples were subsequently post-cured during 2 h at 180°C. Finally, the samples were polished to flat prismatic rectangular shape before the analyses.

Characterization

^{1}H NMR spectra were obtained using a Varian Gemini 400 MHz Fourier-Transform (FT) Nuclear Magnetic Resonance (NMR) spectrometer. In total, 16 scans with a 1.0 s relaxation delay (D1) were averaged over a sampling period of 1 min for the acquisition of the ^{1}H-NMR spectra. $CDCl_3$ was used as solvent and TMS as internal standard.

The kinetics of photopolymerization was determined by real-time (RT) FT-IR spectroscopy, employing a Thermo-Nicolet 5700 FTIR

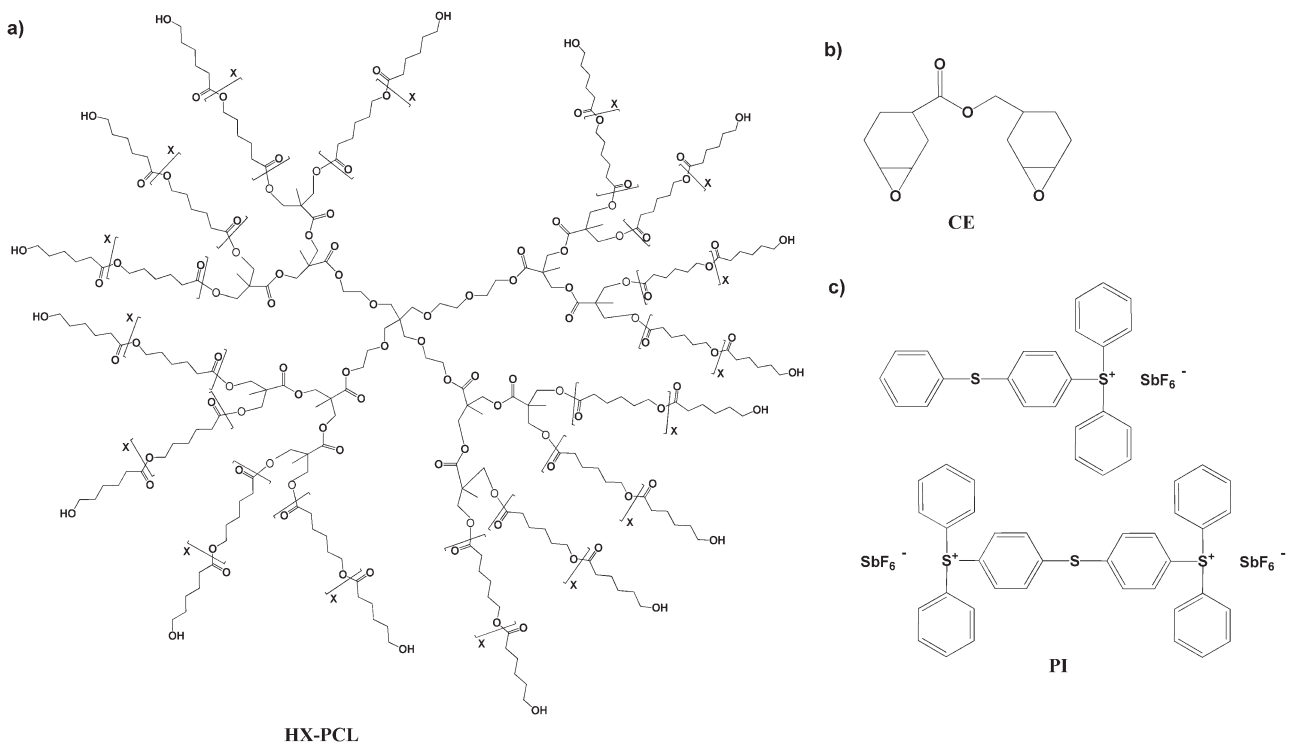

Scheme 2. Chemical structures of (a) idealized multiarm star, (b) bis-cycloaliphatic diepoxy resin (CE), and (c) triphenylsulfonium hexafluoroantimonate (PI).

Table II. Summary of Structural Characteristics and Thermal Properties of the Multiarm Stars

Star	DP_{arm}[a]	PCL_{arms}[b]	M_n[c] (g/mol)	T_g (°C)	T_m (°C)	X_c (%)	$T_{5\%}$[d] (°C)	T_{max}[d] (°C)
H20-PCL	15	11	20600	−54.5	50.7	49.7	302	344
H30-PCL	11	29	38700	−57.6	49.5	48.3	288	347
H40-PCL	16	41	73630	−55.2	51.8	50.2	287	352

[a] Degree of polymerization of the PCL arms (DP_{arm}) determined by ^{1}H NMR spectroscopy.
[b] Average number of PCL arms per molecule determined by ^{1}H NMR spectroscopy.
[c] Average number molecular weight of the obtained stars calculated by ^{1}H-NMR spectroscopy.
[d] Temperature of a 5% of weight loss and maximum rate of weight loss calculated by thermogravimetry.

device. Epoxy group conversion was followed in real-time upon UV exposure, by monitoring the decrease in the bands at 789 and 748 cm^{-1} corresponding to the epoxy ring deformation. A medium pressure mercury lamp equipped with an optical guide was used to induce the photopolymerization (light intensity on the surface of the sample was about 5 mW/cm^{-2}). Variation in the experimental conditions (light intensity, humidity, and temperature) caused slight differences in the kinetic curves. For this reason, all the conversion curves contained in the figures were performed on the same day and under the same conditions and thus good reproducibility was obtained. All the polymerization reactions were performed at room temperature at constant humidity (25–30%). The conversion during photocuring ($\alpha_{UV,FT\text{-}IR}$) was calculated using the following equation:

$$\alpha_{UV,FT-IR} = \frac{1-\overline{A^t}}{\overline{A^0}} \quad (1)$$

where $\overline{A^t}$ is the normalized absorbance of the epoxy band at a given time and $\overline{A^0}$ is the initial absorbance.

DMTA analyses were carried out with a TA Instruments DMA Q800. Single cantilever bending was performed on prismatic rectangular samples. The apparatus was operated dynamically, at 2°C/min, from 40 to 250°C. The frequency of application of the force was 1 Hz and the amplitude of the deformation 10 μm. The T_g value was assumed as the maximum of the loss factor curve (tan δ).

Rheometric measurements were carried out in the parallel plates (geometry of 25 mm) mode with an ARG2 rheometer (TA Instruments, UK, equipped with electrical heated plates, EHP). Complex viscosity (η^*) of the pure multiarm stars was recorded as function of angular frequency (0.05–100 rad/s) with a constant deformation of 50% at 60, 70, and 80°C.

Thermogravimetric analysis (TGA) was performed with a METTLER TGA/SDTA 851 instrument between 30 and 800°C at a heating rate of 10°C/min in air.

The cryofracture of the specimens were done under liquid nitrogen. Afterwards, the samples were metalized with gold and observed by SEM using a scanning electron microscopy Jeol JSM 6400.

The impact test was performed at room temperature by means of a Zwick 5110 impact tester, according to ASTM D4508-10 using rectangular samples. The pendulum employed had a kinetic energy of 1 J.

RESULTS AND DISCUSSION

Synthesis and Characterization of HX-PCL Multiarm Star Polymers

The multiarm star polymers synthesized in this work were prepared by the so-called "core first" strategy using Boltorn type polyesters of different weight as the core. Poly(ε-caprolactone) arms were grown from the hydroxyl groups of the hyperbranched core using $Sn(Oct)_2$ as catalyst.[31] The proportion of ε-CL to OH groups in the polymerization mixture was set to 10 for all the polymers with the objective of obtaining stars with similar arm lengths. However, it was reported that the degree of modification in H40-PCL polymers was lower than expected because not all the OH were able to initiate the polymerization of ε-CL.[32]

To fully characterize the synthesized stars, we determined the degree of polymerization (*DP*) of the arms by ^{1}H NMR spectroscopy. Figure 1 shows as an example the spectrum of H20-PCL with the corresponding assignments. The intensity of the signals 5 and 5′ are commonly used to determine the *DP* of the arms in multiarm stars,[33] but in our case the overlapping of signal 5′ with methylene signals of the core molecule (**B**) did not allow to perform in this way the calculation. Thus, we selected the signal at 2.3 ppm, assigned to the methylene protons 1 and 1′ of the repeating and final ε-caprolactone units and the signal at 4 ppm, assigned to the methylene 5 of the repeating unit. The difference between the former and the latter gave the contribution of the final ε-caprolactone unit. Dividing this value by the intensity of signal 5 and adding the final unit, the *DP* of the ε-caprolactone arms was calculated for each multiarm star. As can be seen in Table II, although this polymerization has a living character and the feed molar ratio ε-CL /OH was 10 in all cases, a higher degree of polymerization than expected was achieved. It can be hypothesized that some OH groups were not able to initiate the polymerization of ε-CL, which could be attributed to the interaction between OH groups by hydrogen bonding or to topological restrictions that rendered some hydroxyl groups inactive. Thus, the following step was to calculate the number of arms in each multiarm star. In order to do so, we used the global intensity of the broad signals corresponding to methyl groups of the core molecule (**C**) at 1–1.3 ppm divided by 3 and the intensity of the signal 5, which corresponds to a methylene in the arms, divided by 2 and by the number of these methylene units in the arm ($DP_{arms} - 1$), and we related them to the number of OH and CH_3 in the core molecule given in the data sheet of Boltorn polyesters. All these calculations are only approximate because the large and highly

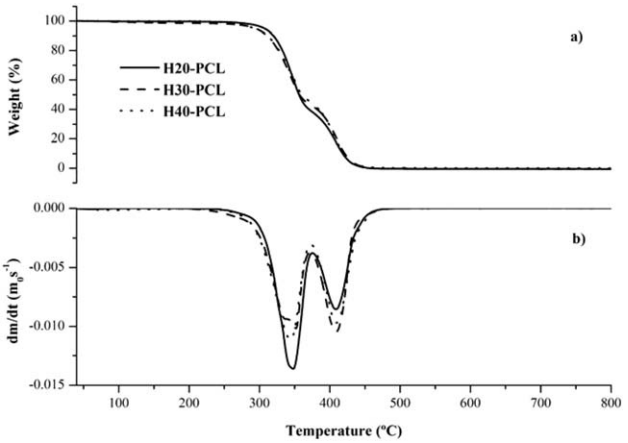

Figure 2. TGA curves of the pure multiarm stars synthesized in N_2 atmosphere.

branched structure of these molecules disturbs the relaxation times of the protons and broadens the signals corresponding to the core structure, but they were comparable to the values obtained by ^{13}C-NMR spectroscopy recorded in quantitative conditions. As observed in Table II, the number of arms was lower than the predicted by the number of OH in the HBP core. Taking into account the arm length, the actual number of arms and the original ε-CL/OH feed ratio, it can be verified that all the ε-CL was polymerized. The number of arms reached a maximum for H30-PCL (29 of 32 possible) and therefore, the arms had a lower DP. From the molecular weight of the core and the number of arms and their DP, average molecular weights in number were calculated for all the synthesized structures and reported in Table II.

Table II also summarizes the most relevant thermal properties of the multiarm stars, determined by calorimetry and thermogravimetry. As can be seen, semicrystalline polymers were obtained in all cases, with similar degrees of crystallinity X_c regardless the differences in DP_{arms}. The values of T_g and T_m were in the range of linear poly(ε-caprolactone). The T_g of the hyperbranched core could not be determined given its small weight proportion in the multiarm stars. No significant differences were observed between the different multiarm stars giving similar values to those measured for poly(ε-caprolactone) multiarm star with hyperbranched poly(glycidol) as the core and arms of a DP_{arm} near to 10.[33] Thus, the influence of the core in the crystalline character of the stars seems to be negligible.

The results of the thermogravimetric analysis of the multiarm stars are summarized in Table II and Figure 2. Table II shows that on increasing the core size, the onset temperature of the decomposition process decreased, but the temperature of the peak of the maximum degradation increased. Figure 2 shows a two-step degradation pattern of the multiarm stars. The ester groups in the arms and core structure experiment degradation by a β-elimination process, giving rise to different fragments that are lost in two different processes. The first step would correspond to the degradation of the arms and the second could be related to the degradation of the core molecule. We verified that the thermal degradation of the HBP core occurred at a temperature similar to the second degradation peak of the multiarm star.

The frequency-dependence of the complex viscosity of the multiarm stars was determined at different temperatures. All formulations showed a Newtonian behavior, with a constant value of complex viscosity in the selected frequency range. Table III collects the complex viscosity of the HX-PCL stars at temperatures of 60, 70, and 80°C. As expected, the viscosity decreased on increasing the temperature. However, there was not a clear dependence on the molecular weight of the star. The viscosity of the multiarm stars depends not only on the molecular weight but also on the DP of the arms, as put into evidence in a previous study.[30] This is also evidenced in the present case, where it is observed that H30-PCL star had an intermediate molecular weight but the viscosity is the lowest because it possessed that shortest arm length, as seen in Table II.

Photocuring Kinetics of CE Resin with Different Proportions of HX-PCL

Cationic photocuring and thermal curing of CE resin with a variety of polymeric modifiers has been studied in the past.[12,16,24,26,27,34,35] The presence of reactive hydroxyl groups in the mixture accelerates the photocuring process because of their participation in the cationic ring-opening of epoxides by the activated monomer (AM) mechanism.[36,37] Decker et al. reported that even the absorbed environmental moisture was capable of accelerating the curing process, making it possible to reach complete cure even at room temperature in dark conditions after photoirradiation.[3] However, one must take into account the concurrence of other factors that have the opposite effect, such as 1) the availability of the reactive hydroxyl groups, depending on the modifier composition, topology, structure and molecular weight, 2) the mobility of the reactive species formed by reaction of the polymeric modifiers and 3) the presence of ether groups in the modifier structure. Therefore, some possibilities arise: a clear accelerative effect can been observed,[12,26] a clearly decelerative effect[24,34] or a complex combined effect depending on the amount of polymeric modifier.[35]

Figure 3 shows that the addition of H20-PCL produced a gradual accelerative effect on the photocuring of the CE resin. It is hypothesized that the catalytic effect of reactive hydroxyl groups is predominant over other structural and composition factors. The addition of H30-PCL and H40-PCL also produced an accelerative effect, but the effect was less gradual as the molecular weight of the modifier increased. If the effect of the different modifiers is compared, it is observed that H40-PCL and H30-PCL produced a stronger effect than H20-PCL, which can be rationalized by 1) the higher amount of available hydroxyl groups of H40-PCL in comparison with H20-PCL in the former

Table III. Complex Viscosity (η^*) of HX-PCL Measured at Different Temperatures

	η^* (Pa·s)		
Temperature (°C)	H20-PCL	H30-PCL	H40-PCL
60	5.64	5.07	6.78
70	3.78	3.31	4.65
80	2.59	2.26	3.09

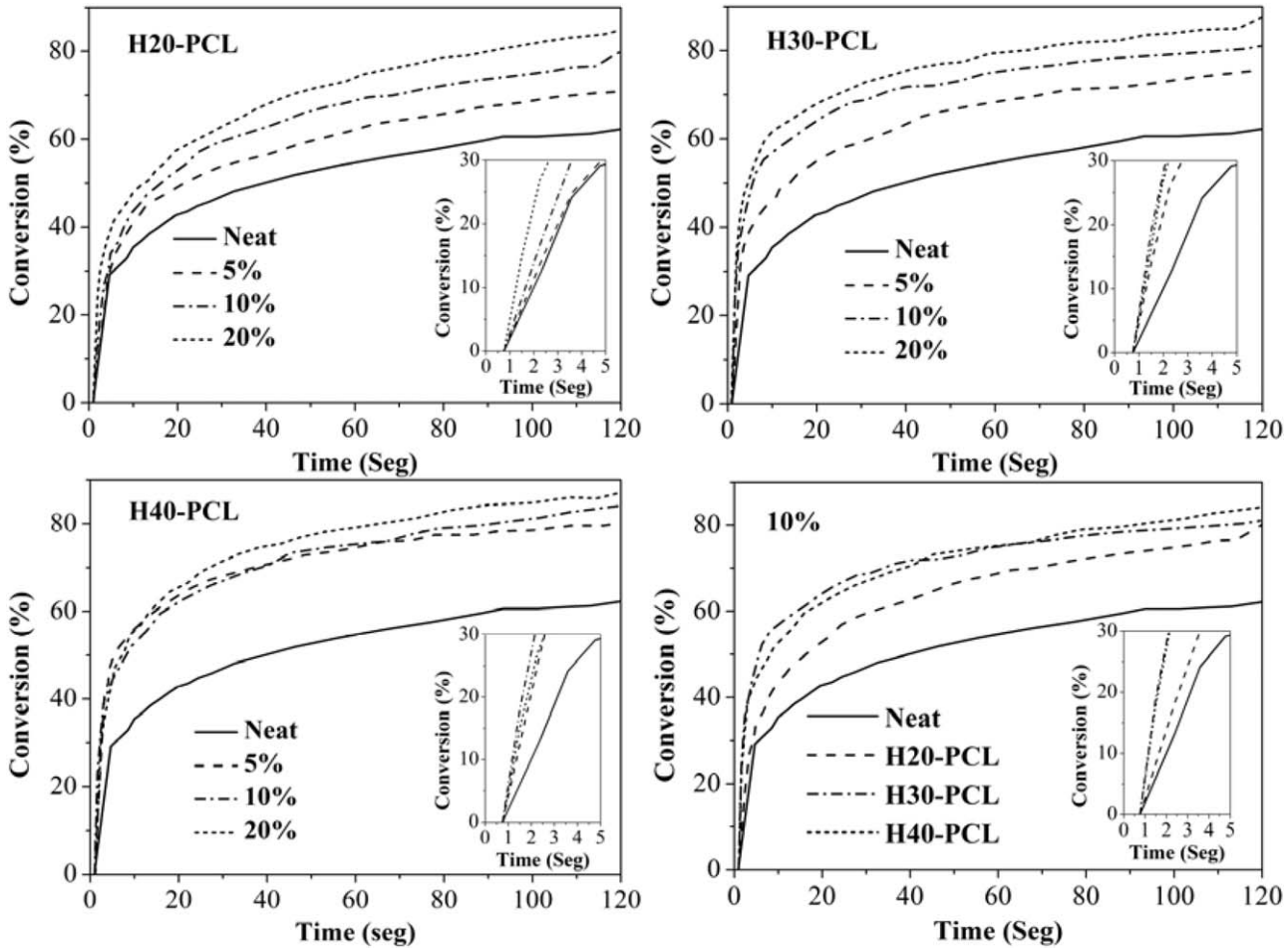

Figure 3. FTIR curves representing conversion as function of irradiation time for neat CE resins and modified formulations with different proportions of H20-PCL, H30-PCL, and H40-PCL and the comparison for the formulations containing a 10% of all the modifiers.

case and 2) the shorter arm length of H30-PCL in comparison with H20-PCL in the latter case, leading to lower mobility restrictions.

Table IV compares the extent of the photocuring process of the different formulations. It is observed how on increasing the amount of modifier, the degree of conversion achieved increased. This effect was more gradual and evident with H20-PCL, in agreement with the effect in the curing kinetics, as discussed above. The samples were not able to reach complete curing because of the occurrence of vitrification, which made it necessary a subsequent thermal postcuring to complete the polymerization. Decker et al.[3] showed that a dark postcuring at room temperature under high relative humidity conditions could lead to complete conversion of epoxy groups, because of the absorption of water and its participation via the AM mechanism, resulting in significant chain termination and transfer processes and a reduction in the crosslinking density of the cured material. In this case, though, the samples for DMA and TGA analysis were postcured shortly after photoirradiation, following the cure schedule described in "Sample Preparation" section in order to overcome vitrification and achieve complete curing, and to maximize the crosslinking density and the T_g.

Table IV. Conversion of Epoxy Groups from FTIR Spectra after Photocuring ($\alpha_{UV,FTIR}$) and Thermal Mechanical Data of the Prepared Thermosets

Sample	$\alpha_{UV,FTIR}$ (%)	Tan δ (°C)	$T_{5\%}$ (°C)
Neat	63	186	324
H20-PCL (%)			
5	72	168	298
10	80	162	301
20	85	145	324
H30-PCL (%)			
5	75	152	309
10	80	151	292
20	88	150	291
H40-PCL (%)			
5	80	173	265
10	84	153	302
20	87	146	298

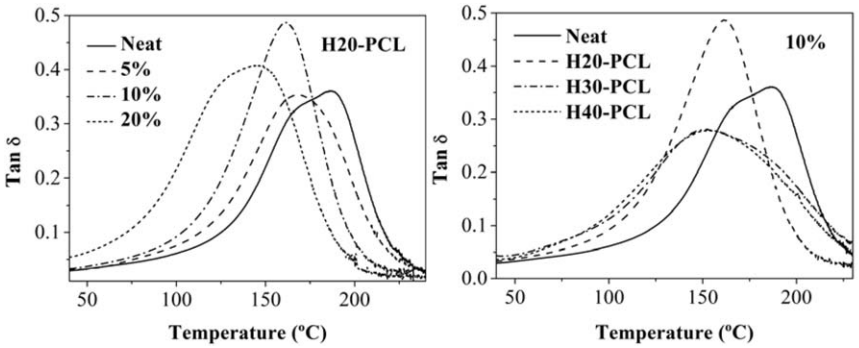

Figure 4. Tan δ against temperature for the neat and modified materials with different proportions of H20-PCL (left) and 10% of all the modifiers (right).

Thermal and Thermomechanical Properties of the Thermosets

The glass transition temperature of the cured materials was determined by DMTA, as the peak temperature of tan δ. The plot of tan δ against temperature is represented in Figure 4 and the peak temperature is reported in Table IV.

The addition of either modifier produced a gradual decrease in glass transition temperature, as illustrated as for H20-PCL in Figure 4. It is observed a shift down to lower temperatures of the tan δ peak, which is an indicative of the mechanical relaxation of the network and is closely related with the glass transition. This is not as clearly deduced from the data shown in Table IV. Indeed, the tan δ curves broadened with the addition of the modifiers, especially H30-PCL and H40-PCL, which made it difficult to determine a nominal value of T_g and put into evidence a somewhat heterogeneous network structure with a disperse distribution of crosslinking density that may be caused by the covalent incorporation of the modifier into the network structure.

Similar results were obtained for cationic cured DGEBA formulations using a multiarm star with a hyperbranched poly(glycidol) core,[29] and using H30 as modifier.[38] First of all, one must take into account the high solubility of PCL in epoxy matrices, especially in cycloaliphatic formulations, which makes it possible to obtain homogeneous materials. Second, the terminal hydroxyl groups of the PCL arms can form covalent linkages with the network structure due to their participation in the cationic curing of epoxides by the AM mechanism.[36] When a hydroxyl group reacts with a tertiary oxonium cation, the chain growth is stopped and a proton is transferred to a monomer, which turns into a secondary oxonium cation that can propagate the polymerization, generating in turn another hydroxyl group. In consequence, the participation of the end hydroxyl groups of the PCL arms in the curing may result in a decrease in crosslinking density and a loosening of the network structure, thus resulting in a decrease in glass transition temperature.

However, the calculated T_g values using a standard rule of mixtures such as the Fox equation (results not shown) were significantly lower than the experimental ones. Such deviations are commonly observed in phase-separated modified thermosets[15] but they are also present in homogeneous materials, as we recently reported.[39] The materials were homogeneous, as was confirmed later by SEM microscopy and, indeed, no secondary relaxation corresponding to the appearance of a second phase at low temperatures was observed. It can be hypothesized that the incorporation of the modifiers into the network structure produced significant mobility restrictions arising from the highly crosslinked hyperbranched core and the presence of physical entanglements between the poly(ε-caprolactone) arms and the crosslinked thermosetting network, as reported previously for poly(ethyleneimine) modified hybrid epoxy networks.[39]

Figure 5 compares the thermal stability of the obtained materials and the characteristic temperatures of 5% weight, $T_{5\%}$, are reported in Table IV. It was expected a certain decrease in thermal stability on increasing the proportion of star in the formulation, caused by the growing amount of ester groups in the modifier. However, Table IV shows no well-defined trend in $T_{5\%}$. In Figure 5 it is observed, overall, that the use of the different modifiers somewhat increased the thermal stability of the cured materials, especially on increasing the molecular weight of the modifier. Indeed, with H20-PCL only the material with a proportion of

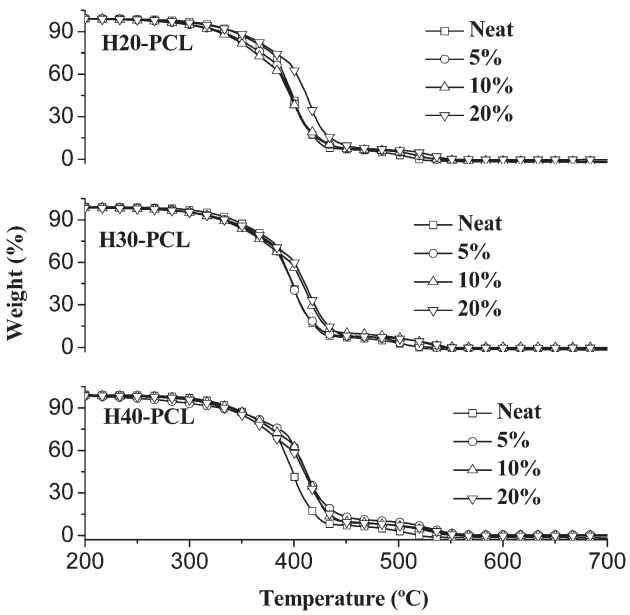

Figure 5. TGA curves for the different materials obtained at 10°C/min under air atmosphere.

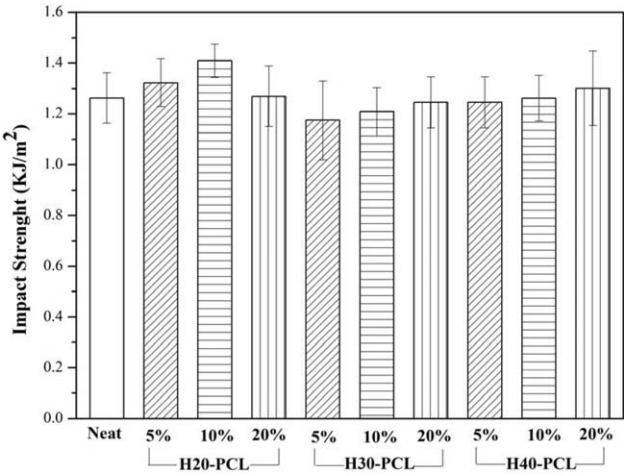

Figure 6. Impact strength dependence of thermosets containing different amounts of the modifiers.

20% of the modifier had a higher thermal stability, whereas with H40-PCL a 5% of the modifier was sufficient to increase the thermal stability.

Mechanical Properties of the HX-PCL Modified Thermosets

We recently demonstrated that multiarm PCL stars with hyperbranched poly(glycidol) core could improve the impact strength of cationic epoxy thermosets to a higher extent than linear PCL, while retaining better thermomechanical properties.[29] Multiarm PCL stars with hyperbranched poly(ethyleneimine) core have also been synthesized and used in anionic epoxy formulations, with a positive effect on impact strength depending on the arm length and hyperbranched core size.[30] Figure 6 shows the results of the impact strength measurements of the neat and modified formulations. An optimum effect with 10% of H20-PCL was obtained, although the net increment is small.

It is acknowledged that hyperbranched polymers that undergo phase separation during curing are capable of producing a significant enhancement in impact strength[9,11,15,16] due to the stress concentration in the area surrounding the particles and an effective stress transfer to the particles, leading to the activation of several energy absorption mechanisms such as shear yielding of the matrix in the vicinity of the particles and cavitation of the particles. In homogeneous systems, an *in situ* reinforcing mechanism caused by a loosening and flexibilization of the network structure is held accountable for, most of the times, a discrete enhancement in impact strength.[40] An enhancement in impact strength has been reported for UV-cured cationic epoxy formulations modified with hyperbranched polymers undergoing phase separation during curing[27] but a certain improvement has also been observed in homogeneous materials.[12,26] In previous works,[15,16] we observed that an excessive compatibility between the modifier and the polymeric modifier prevented phase separation and therefore the toughening effect was very limited. In this case, homogeneous materials were obtained, therefore one could only expect such a modest increase in toughness, produced by an *in situ* reinforcement.

In Figure 7, the SEM micrographs of the fracture surfaces of the neat and modified material with H20-PCL after impact tests are shown. As suggested previously in "Thermal and Thermomechanical Properties of the Thermosets" section 3.3, homogeneous materials were obtained, without evident traces of phase separation From the smooth fracture surfaces it can also be inferred that all the materials had a similar brittle fracture, which was to be expected taking into account the above reported values of impact strength. The fracture surfaces appeared to be only slightly rougher in the case of the modified materials, indicating a somewhat enhanced matrix shear yielding in agreement with the discrete enhancement in toughness discussed above.

CONCLUSIONS

Multiarm star copolymers were synthesized by cationic ring-opening polymerization of ε-caprolactone from hyperbranched aliphatic polyesters of different molecular weight as a core. These multiarm star polymers obtained were used as polymeric modifiers of UV-cured cycloaliphatic epoxy resin.

The presence of these modifiers accelerated the photocuring process because of the participation of the end hydroxyl groups of the poly(ε-caprolactone) arms in the cationic curing of epoxides by the activated monomer (AM) mechanism. The effect was more significant with the higher molecular weight modifier (H40-PCL) than with the lower molecular weight modifier (H20-PCL).

Homogeneous materials were obtained, with a modest decrease of the glass transition temperature because of the incorporation of the modifiers into the network structure and the subsequent loosening and flexibilization of the network structure.

Only H20-PCL had a measurable positive effect on the impact strength of the modified thermosets, while the others did not produce a clear decrease or increase in this property. This discrete effect arises from the fact that the materials are homogeneous and only an *in situ* reinforcement of the matrix may take place.

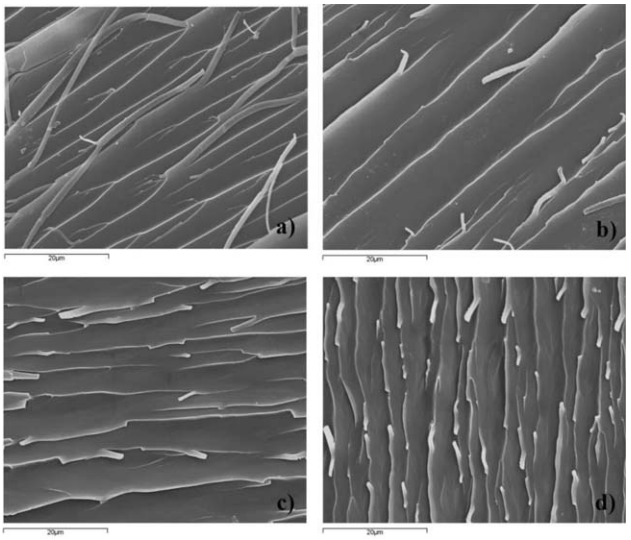

Figure 7. SEM micrographs of the fracture surface of the (a) neat material and modified materials with (b) 5%, (c) 10%, and (d) 20% of H20-PCL.

ACKNOWLEDGMENTS

The authors would like to thank MINECO (MAT2011-27039-C03-01, MAT2011-27039-C03-02) and Generalitat de Catalunya (2009-SGR-1512) for giving financial support. MF acknowledges the grant BES-2009–025226 and XF-F acknowledges the contract JCI-2010-06187. Perstorp is acknowledged for kindly providing Boltorn HBPs.

REFERENCES

1. May, C. A., Ed. Epoxy Resins: Chemistry and Technology; Marcel Dekker: New York, **1988**.
2. Petrie, E. M., Epoxy Adhesive Formulations; McGraw-Hill: New York, **2006**.
3. Decker, C.; Nguyen, T.; Viet, T.; Thi, H. P., *Polym. Int.* **2001**, *50*, 986.
4. Decker, C.; Nguyen Thi Viet, T.; Decker, D.; Weber-Koehl, E. *Polymer* **2001**, *42*, 5531.
5. Crivello, J. V.; Acosta Ortiz, R. *J. Polym. Sci. Part A: Polym. Chem.* **2001**, *39*, 2385.
6. Crivello, J. V. *J. Polym. Sci. Part A: Polym. Chem.* **1999**, *37*, 4241.
7. Bagheri, R.; Marouf, B. T.; Pearson, R. A. *Polym. Rev.* **2009**, *49*, 201.
8. Zheng, S. In *Epoxy polymers: New materials and Innovations*; Pascault, J.-P.; Williams, R. J. J., Eds.; Wiley-VCH: Weinheim, **2010**, Chapter 5.
9. Boogh, L.; Pettersson, B.; Manson, J.-A. E. *Polymer* **1999**, *40*, 2249.
10. Ratna, D.; Simon, G. P. *Polymer* **2001**, *42*, 8833.
11. Ratna, D.; Varley, R.; Simon, G. P. *J. Appl. Polym. Sci.* **2003**, *89*, 2339.
12. Sangermano, M.; Malucelli, G.; Bongiovanni, R.; Priola, A.; Harden, A. *Polym. Int.* **2005**, *54*, 917.
13. Zhang, D.; Jia, D. *J. Appl. Polym. Sci.* **2006**, *101*, 2504.
14. Voit, B.; Lederer, A. *Chem. Rev.* **2009**, *109*, 5924.
15. Flores, M.; Fernández-Francos, X.; Ferrando, F.; Ramis, X.; Serra, A. *Polymer* **2012**, *53*, 5232.
16. Flores, M.; Morell, M.; Fernández-Francos, X.; Ferrando, F.; Ramis, X.; Serra, À. *Eur. Polym. J.* **2013**.
17. Tripathi, G.; Srivastava, D. *Adv. Polym. Technol.* **2007**, *26*, 258.
18. Tripathi, G.; Srivastava, D. *J. Appl. Polym. Sci.* **2009**, *114*, 2769.
19. Iijima, T.; Fujimoto, K. I.; Tomoi, M. *J. Appl. Polym. Sci.* **2002**, *84*, 388.
20. Zhang, X.; Xu, W.; Xia, X.; Zhang, Z.; Yu, R. *Mater. Lett.* **2006**, *60*, 3319.
21. Zhang, X.-H.; Zhang, Z.-H.; Xu, W.-J.; Chen, F.-C.; Deng, J.-R.; Deng, X. *J. Appl. Polym. Sci.* **2008**, *110*, 1351.
22. Gao, N.; Liu, W.; Ma, S.; Tang, C.; Yan, Z. *J. Polym. Res.* **2012**, *19*, 9923.
23. Ochi, M.; Ichikawa, N.; Harada, M.; Hara, M.; Uchida, H. *J. Appl. Polym. Sci.* **2012**, *124*, 4572.
24. Dabritz, F.; Voit, B.; Naguib, M.; Sangermano, M. *Polymer* **2011**, *52*, 5723.
25. Sangermano, M.; Messori, M.; Galleco, M. M.; Rizza, G.; Voit, B. *Polymer* **2009**, *50*, 5647.
26. Sangermano, M.; Priola, A.; Malucelli, G.; Bongiovanni, R.; Quaglia, A.; Voit, B.; Ziemer, A. *Macromol. Mater. Eng.* **2004**, *289*, 442.
27. Sangermano, M.; Malucelli, G.; Bongiovanni, R.; Priola, A.; Harden, A.; Rehnberg, N. *Polym. Eng. Sci.* **2003**, *43*, 1460.
28. Karger-Kocsis, J.; Frohlich, J.; Gryshchuk, O.; Kautz, H.; Frey, H.; Mülhaupt, R. *Polymer* **2004**, *45*, 1185.
29. Morell, M.; Ramis, X.; Ferrando, F.; Serra, A. *Polymer* **2011**, *52*, 4694.
30. Acebo, C.; Fernandez-Francos, X.; Ferrando, F.; Serra, A.; Salla, J. M.; Ramis, X. *React. Funct. Polym.* **2013**, *73*, 431.
31. Trollsäs, M.; Hedrick, J. L.; Mecerreyes, D.; Dubois, P.; Jerome, R.; Ihre, H.; Hult, A. *Macromolecules* **1997**, *30*, 8508.
32. Chen, S.; Zhang, X.-Z.; Cheng, S.-X.; Zhuo, R.-X.; Gu, Z.-W. *Biomacromolecules* **2008**, *9*, 2578.
33. Morell, M.; Lederer, A.; Ramis, X.; Voit, B.; Serra, A. *J. Polym. Sci. Part A: Polym. Chem.* **2011**, *49*, 2395.
34. Foix, D.; Fernández-Francos, X.; Ramis, X.; Serra, À.; Sangermano, M. *React. Funct. Polym.* **2011**, *71*, 417.
35. Morancho, J. M.; Cadenato, A.; Ramis, X.; Fernandez-Francos, X.; Flores, M.; Salla, J. M. *J. Therm. Anal. Calorim.* **2011**, *105*, 479.
36. Kubisa, P.; Penczek, S. *Prog. Polym. Sci. (Oxford)* **1999**, *24*, 1409.
37. Crivello, J. V.; Liu, S. *J. Polym. Sci. Part A: Polym. Chem.* **2000**, *38*, 389.
38. Fernández-Francos, X.; Salla, J. M.; Cadenato, A.; Morancho, J. M.; Serra, A.; Mantecón, A.; Ramis, X. *J. Appl. Polym. Sci.* **2009**, *111*, 2822.
39. Fernández-Francos, X.; Santiago, D.; Ferrando, F.; Ramis, X.; Salla, J. M.; Serra, À.; Sangermano, M. *J. Polym. Sci. Part B: Polym. Phys.* **2012**, *50*, 1489.
40. Fu, J.-F.; Shi, L.-Y.; Yuan, S.; Zhong, Q.-D.; Zhang, D.-S.; Chen, Y.; Wu, J. *Polym. Adv. Technol.* **2008**, *19*, 1597.